Search for intermediate structure in the $^{19}F + ^{12}C$ system

G. Vourvopoulos
Department of Physics and Astronomy, Western Kentucky University, Bowling Green, Kentucky 42101

C. F. Maguire and Z. Kui
Department of Physics and Astronomy, Vanderbilt University, Nashville, Tennessee 37203

L. C. Dennis, K. W. Kemper, and D. P. Sanderson
Department of Physics, Florida State University, Tallahassee, Florida 32305

(Received 27 June 1986)

The reaction $^{12}C(^{19}F,\alpha)^{27}Al$ was studied over the same energy range, $E_{c.m.}=16$–22 MeV, where previous elastic and inelastic measurements were found to exhibit large back angle oscillatory motion. Excitation functions and angular distributions were measured for a number of alpha particle groups. These excitation functions do not show a strong correlation among themselves, nor do they correlate strongly with the elastic and inelastic scattering data. The angular distributions for two resolved states and two unresolved groups have the same average slope without any discernible pattern. Hauser-Feshbach calculations are structureless and the calculated angular distributions have a much smaller slope than the data. Overall, we conclude that within the present study it has not been possible to identify unequivocally any resonances in the $^{12}C+^{19}F$ system.

I. INTRODUCTION

In a recent experiment,[1] the back angle elastic scattering of $^{19}F + ^{12}C$ revealed three prominent gross structures at $E_{c.m.}=18.0$, 20.7, and 22.1 MeV. Angular distributions at the above energies indicate that the structures are dominated by single l values, namely $l=14$, 16, and 17, respectively. Such an enhancement of back angle elastic scattering has been observed for a number of other heavy-ion pairs with a total mass number $M>32$.[2] The interpretation of these anomalies has not been the same through the literature, although for a number of cases they have been presented as evidence for nuclear molecular behavior.

In general, anomalies observed in one channel only, need further supportive evidence if they are to be considered as molecular resonances. As an example, in the case of the $^{16}O+^{28}Si$ system and in the energy region close to the Coulomb barrier,[3] the elastic scattering excitation function at $\theta_{c.m.}=180°$ indicates two deep minima. The authors of Ref. 3 fit the data with an optical model that has a conventional imaginary potential but a real potential that is repulsive at short distances and very attractive at the nuclear surface. These calculations predict the deep minima in the excitation function to be associated with a sharp fall at $\theta_{c.m.}=180°$ in the angular distribution, a result that is experimentally verified. The correlation of deep minima in the excitation function with minima at 180° as well as the rises at 180° seen near maxima in the excitation function, are claimed to arise from resonance-background interference. As such, they are strong evidence for molecularlike structures. In the case of the $^{12}C+^{28}Si$ system, the backward rise is not confined to the elastic channel but shows up in inelastic scattering and in few-nucleon transfer reactions.[4] The angular distributions for the total reaction yield at large angles follow a $1/\sin\theta_{c.m.}$ relation. Such behavior is expected in the classical limit for the decay of a rapidly rotating molecular system.

For the case of the $^{19}F+^{12}C$ system,[1] the maxima in the excitation function ($E_{c.m.}=18.0$, 20.7, 22.1 MeV) correlate with maxima at $\theta_{c.m.}=180°$ in the angular distributions. Data, however, taken at a minimum fail to show any oscillations like those seen in the $^{16}O+^{28}Si$ system. Neither does a minimum become apparent at $\theta_{c.m.}=180°$.

The present experiment was performed in order to see whether the anomalies observed in the elastic scattering data for the $^{19}F+^{12}C$ system persist in other channels too. The $^{12}C(^{19}F,\alpha)^{27}Al$ reaction was studied over the same c.m. energy range as the elastic scattering, measuring excitation functions, and angular distributions for a number of alpha groups.

II. EXPERIMENTAL PROCEDURE

The super-FN Tandem accelerator of Florida State University was utilized in taking the data. An excitation function for the reaction $^{12}C(^{19}F,\alpha)^{27}Al$ was taken in the energy range 41.0–57.0 MeV ($E_{c.m.}=16$–22 MeV) in steps of 400 keV. The target was a 50 $\mu g/cm^2$ C foil, corresponding to an energy loss of 350 keV for a 40 MeV F beam. A wedge with six single surface barrier detectors covered the angles between 8° and 53° in steps of 9°. Al foil was placed in front of the detectors to stop ions heavier than α particles. Collimators in front of the detectors subtended an angle of $\Delta\theta=\pm1.25°$. For the angular distributions, the same setup was used and the wedge was placed at two settings so that angles between 8° and 71° ($\theta_{c.m.}=10.9°$–$91.2°$) were covered. For the latter measurements, the target thickness was increased to 100 $\mu g/cm^2$.

An energy spectrum from the most forward detector is shown in Fig. 1. The energy resolution of the system was not adequate to resolve all low lying excited states. Except for the ground state and the 2.21 MeV state of ^{27}Al which were resolved, the remaining energy groups contain two or three energy levels. This does not hamper the analysis of the excitation functions since results are sought indicating correlations among many channels. A total of 30 excitation functions were obtained over five α groups and six angles, but only 18 of them contained statistically meaningful results to be analyzed. Figure 2 shows excitation functions of different α groups at the same angle and Fig. 3 shows excitation functions of the same α group at different angles. Although a number of prominent peaks are observed in individual excitation functions, the present data fail to show in a coherent fashion the prominent structures that were observed in the elastic scattering.

III. ANALYSIS

A. Excitation functions

The measured excitation functions were analyzed using statistical criteria. For this purpose, correlation and deviation functions were computed. The absolute correlation function

$$C(E)=\frac{2}{N(N-1)}\sum_{\substack{i=1\\ j>i}}^{N}|C_{ij}(E)|$$

and the correlation function

$$C'(E)=\frac{2}{N(N-1)}\sum_{\substack{i=1\\ j>i}}^{N}C_{ij}(E)$$

test the degree of correlation among the measured excitation functions. In the above formulae, N denotes the number of excitation functions, and the $C_{ij}(E)$'s are the normalized cross-correlation functions defined as

$$C_{ij}=\frac{\langle\sigma_i(E)\sigma_j(E)\rangle-\langle\sigma_i(E)\rangle\langle\sigma_j(E)\rangle}{\{[\langle\sigma_i^2(E)\rangle-\langle\sigma_i(E)\rangle^2][\langle\sigma_j^2(E)\rangle-\langle\sigma_j(E)\rangle^2]\}^{1/2}}\ .$$

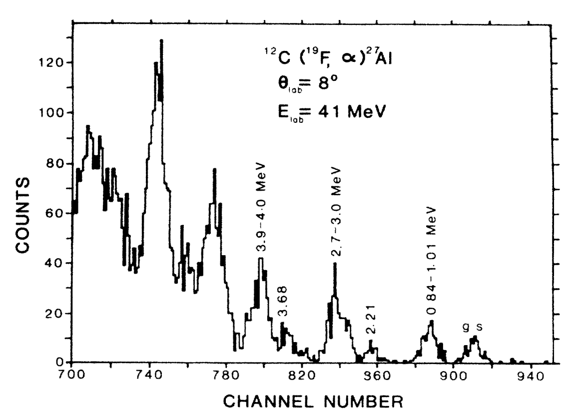

FIG. 1. Spectrum of alpha particles from the reaction $^{12}C(^{19}F,\alpha)^{27}Al$.

The absolute deviation function

$$D(E)=\frac{1}{N}\sum_{i=1}^{N}\left|\frac{\sigma_i(E)}{\langle\sigma_i(E)\rangle}-1\right|$$

and the deviation function

$$D'(E)=\frac{1}{N}\sum_{i=1}^{N}\frac{\sigma_i(E)}{\langle\sigma_i(E)\rangle}-1$$

furnish information on the relative strength of anomalies. $\langle\sigma_i(E)\rangle$ represents the average cross section over a running averaging interval ΔE.

The statistical analysis was performed on 18 excitation functions. There is an implicit dependence of the correlation and deviation functions on the average interval width. This is not a very strong dependence, however, and variation of the ΔE interval between $\Delta E_{\rm lab}=3$ and 6 MeV did not present any serious alteration of the deviation function. Thus, Fig. 4 shows the correlation and deviation functions calculated with a running average interval of $\Delta E_{\rm lab}=3.2$ MeV.

Both deviation functions (normal and absolute) show a

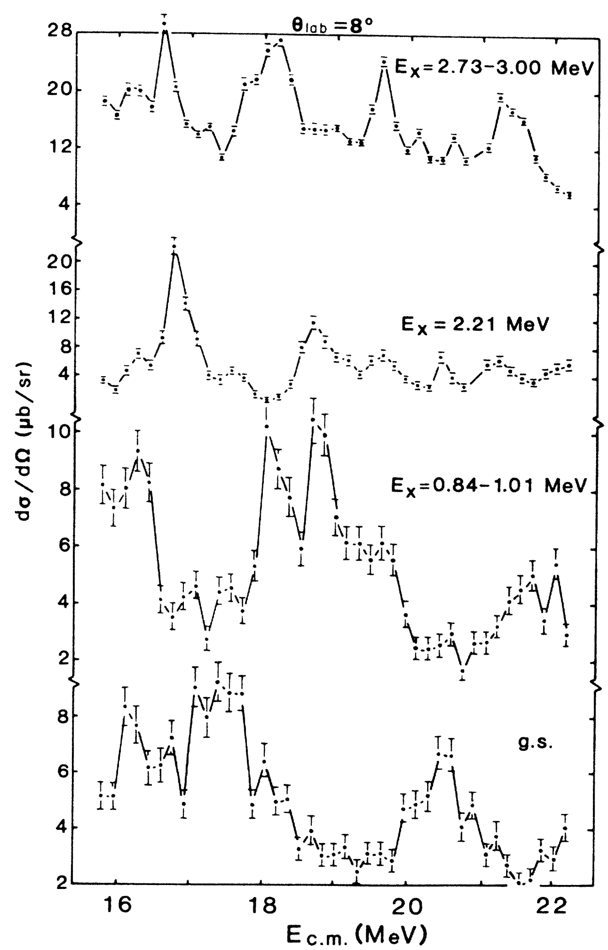

FIG. 2. Excitation functions of alpha groups from the reaction $^{12}C(^{19}F,\alpha)^{27}Al$ at $\theta_{\rm lab}=8°$. Solid lines are for guiding the eye.

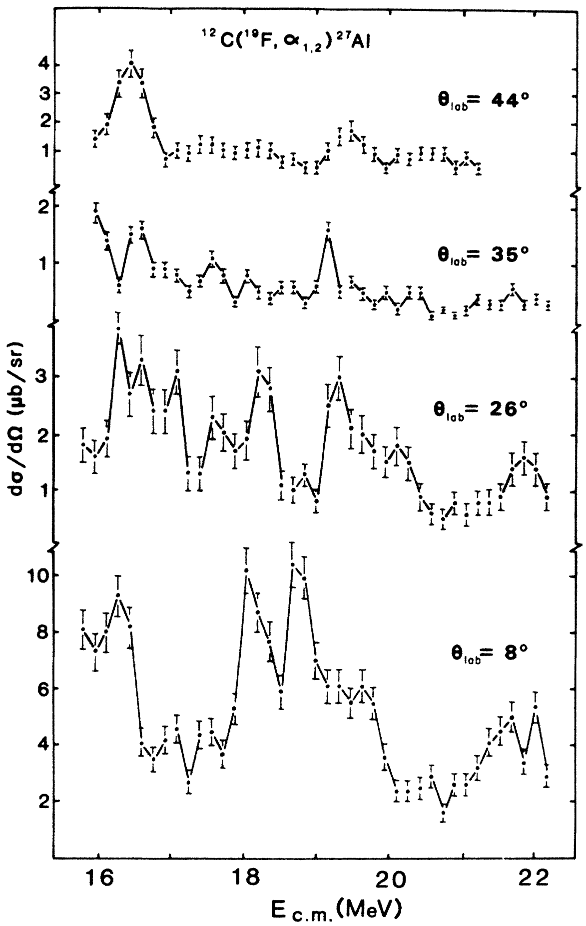

FIG. 3. Excitation functions for the $E_x = 0.84-1.01$ MeV α group from the $^{12}C(^{19}F,\alpha)^{27}Al$ reaction, measured at different laboratory angles. Solid lines are for guiding the eye.

number of structures, but they are all small and do not correlate with the broad structures observed in the elastic scattering. There is only one anomaly at 16.2 MeV that shows a somewhat larger deviation, and both the elastic and inelastic scattering data show a sharp minimum at approximately the same energy. The 1% probability limit is also plotted in Fig. 4. It represents the deviation from the average value for which the probability of finding a larger deviation is 1%. This limit has been calculated using the probability distribution

$$P(y_k) = \left[\frac{n_k}{1-d_k}\right]^{n_k} y_k^{n_k-1} \exp\left[-n_k \frac{y_k+d_k}{1-d_k}\right] \times \frac{I_{n_k-1}[2n_k(y_k d_k)^{1/2}/1-d_k]}{[n_k(y_k d_k)^{1/2}/1-d_k]^{n_k-1}} ,$$

where n_k is the number of independent channels in the reaction, d_k the direct reaction contribution, and I_n the modified Bessel function of order n. For a detailed description of the evaluation of the probability distribution see Ref. 5.

The comparison between the distribution of calculated values of $D'(E)$ and the theoretical probability distribution for the same quantity is shown in Fig. 5. No significant discrepancies from statistical predictions are observed.

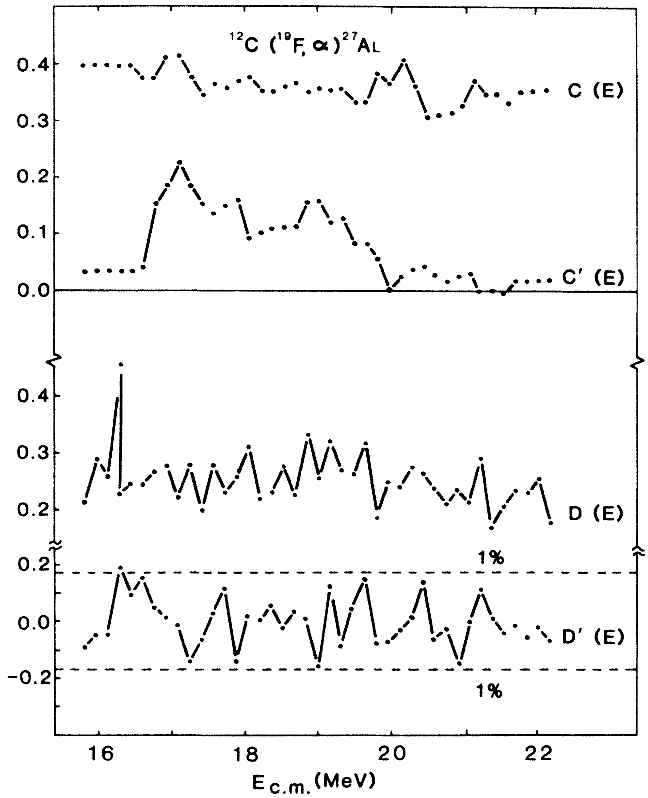

FIG. 4. Results of the statistical analysis on 18 excitation functions. $C(E)$, $C'(E)$, $D(E)$, and $D'(E)$ denote the absolute correlation function, the correlation function, the absolute deviation function, and the deviation function, respectively. The dashed lines on the deviation function indicate the 1% probability limit.

The correlation function $C'(E)$ indicates three maxima at $E_{c.m.} = 17$, 17.9, and 19 MeV. The standard deviation for $C'(E)$ due to the finite range of data is given by[5]

$$\sigma_{C'} = \left[\frac{2}{N(N-1)(\eta-1)}\right]^{1/2} ,$$

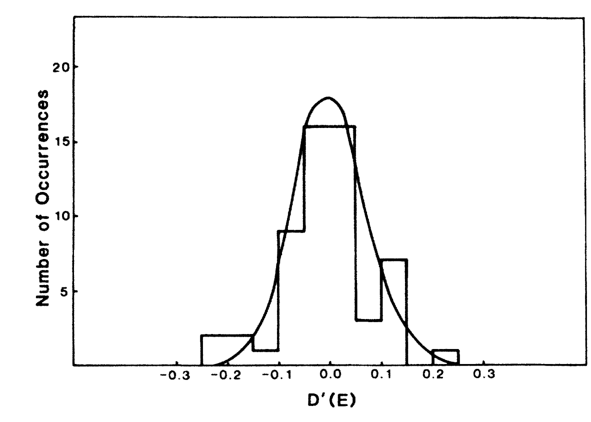

FIG. 5. Histogram of the calculated values for the deviation function $D'(E)$ along with the theoretical probability distribution.

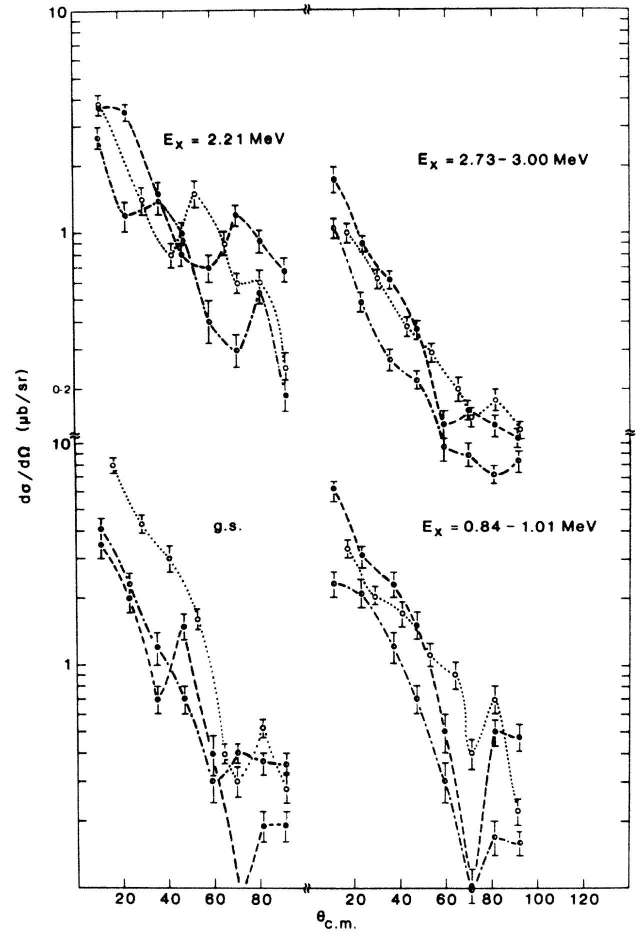

FIG. 6. Angular distributions for two resolved states and two unresolved groups from the reaction $^{12}C(^{19}F,\alpha)^{27}Al$. Drawn lines are to guide the eye. Dotted lines and open circles are for $E_{c.m.}=17.4$ MeV; dashed lines and full circles are for $E_{c.m.}=19.3$ MeV; dot-dashed lines and semifull circles are for $E_{c.m.}=20.1$ MeV.

where N is the number of excitation functions and η is the number of data points in the averaging interval. For the present set of data $\sigma_{C'}=0.03$. For an uncorrelated statistical ensemble, the values of $C'(E)$ are expected to fall inside the limit $3\sigma_{C'}=0.1$. Therefore the observed maxima with values 0.25, 0.15, and 0.15 are outside the statistical limits.

In conclusion, although an anomaly in the deviation function at 16.2 MeV and anomalies in the correlation function at 17, 17.9, and 19 MeV are observed outside accepted statistical limits, they do not correlate with the structures observed in the elastic scattering.

B. Angular distributions

Angular distributions were measured at five energies ($E_{c.m.}=17.0$, 17.4, 18.5, 19.3, 20.1 MeV) and over the angular range $\theta_{c.m.}=10°–90°$. The energies were chosen to correspond to positions in the excitation function where either prominent peaks appear for some levels or maxima occurred in the back angle elastic scattering. Figure 6 displays the angular distributions for two resolved states (the g.s. and the 2.21 MeV state) and two unresolved groups (0.84—1.01 MeV and 2.73—3.0 MeV). No particular pattern emerges from these angular distributions and any fluctuations that might be perceived as oscillations have their maxima quite far removed from each other. They correspond to l values much smaller than those observed in the elastic scattering.

It should be pointed out that although one l value can contribute in the entrance channel for a given j^{π} of a resonance ($j^{\pi}=\frac{1}{2}^{+}$ for the ^{19}F g.s.), for the exit channels considered, a number of outgoing partial waves can be coupled coherently to produce the differential cross section. It becomes therefore quite difficult to assign an l value based on the shape of the angular distributions.

A common feature in all angular distributions is the same average slope over the measured angular range. Since the slope in the forward angles follows nearly a $1/\sin\theta$ relation, and compound nucleus formation is assumed to be of importance in the range of energies studied, Hauser-Feshbach calculations were performed.

IV. HAUSER-FESHBACH CALCULATIONS

The Hauser-Feshbach calculations were performed with the computer code HELGA (Ref. 6) over the same energy range as that covered by the experiment. Listed in Table I are the channels that were thought to be most important in the statistical decay of the compound nucleus ^{31}P, and the optical model parameters used in the calculations. The maximum entrance channel orbital angular momentum and the maximum compound nucleus spin were adjusted at each incident energy so that the calculated fusion

TABLE I. Optical model parameters used for the Hauser-Feshbach calculations.

System	V_r (MeV)	r_0 (fm)	a_r (fm)	W_i (MeV)	r_{0i} (fm)	a_i (fm)	Ref.
$^{19}F+^{12}C$	19.6	1.24	0.616	4.6 (vol)	1.38	0.772	7
$^{16}O+^{15}N$	105.7	1.16	0.526	9.7 (vol)	1.16	0.526	8
$n+^{30}P$	$47.01-0.267E-0.0018E2$	1.305	0.66	$9.52-0.053E$(surf)	1.256	0.48	9
$p+^{30}Si$	$55.3-0.55E$	1.25	0.65	13.5 (surf)	1.25	0.47	9
$\alpha+^{27}Al$	51.2	1.655	0.588	11.87 (vol)	1.655	0.588	10
$^{8}Be+^{23}Na$	38.3	1.16	0.59	62.03 (vol)	0.86	0.87	11,12
$^{6}Li+^{25}Mg$	32.59	1.725	0.724	24.99 (vol)	1.682	0.886	13
$^{7}Li+^{24}Mg$	53.2	1.22	0.57	38.7 (vol)	1.27	1.26	14

TABLE II. Experimental and calculated total fusion cross sections and maximum entrance channel l values.

$E_{c.m.}$ (MeV)	σ_{exp} (mb)[a]	σ_{calc} (mb)	l_{cutoff}
16.2	930	972	13
17.4	975	960	13
18.6	1020	1025	14
20.1	1080	1087	15

[a]Reference 15.

cross section was differing less than 5% from the measured fusion cross section.[15] Table II indicates the relevant information on fusion cross section and maximum entrance channel orbital angular momentum for four energies within the range of the present experiment. The level density parameters for the residual nuclei are listed in Table III. They were obtained using the fitting procedure prescribed by Gilbert and Cameron.[16] For each of the residual nuclei used in the calculation the total number of low lying states below a given excitation energy was fitted to the integral of a simple exponential form of the level density. This simple level density form is then matched to the Fermi gas level density in slope and magnitude by adjusting the level density parameter a and the excitation energy where the two forms of the level densities are matched. The spin cutoff parameter was obtained from the level density parameter using the formula $\sigma^2 = 0.1459\sqrt{aU}A^{2/3}$. This formula was given by Gilbert and Cameron but uses the corrected numerical factor of Facchini and Saetta-Menichella.[17] The pairing energies were taken from Cameron and Elkin.[18]

Since a small (20%) variation of the level-density parameter can lower the cross section of a discrete state by a factor ~ 4.5, no attempt was made to normalize the calculations. The cross section ratio $\sigma_{exp}(\text{g.s.})/\sigma_{exp}(2.21\text{ MeV})$ is within 10% of the calculated ratio $\sigma_{calc}(\text{g.s.})/\sigma_{calc}(2.21\text{ MeV})$. Figure 7 shows the angular distributions of the g.s. and 2.21 MeV states in ^{21}Al averaged over the energy region of the experiment along with the calculated compound nucleus cross section averaged over the same energy region. The calculated cross section is approximately a factor of 2 less than the experimental cross section. Since an absolute magnitude of the calculated compound nucleus cross section cannot be obtained, we can only compare shapes of angular distributions. A feature of the calculated cross section is the total lack of any oscillations, a feature not very dissimilar from what is experimentally observed. The calculated slope, however, is quite different from what is experimentally found. The Hauser-Feshbach calculation follows a $1/\sin\theta$ distribution, while both the g.s. and the 2.21 MeV state have the same but much steeper slope.

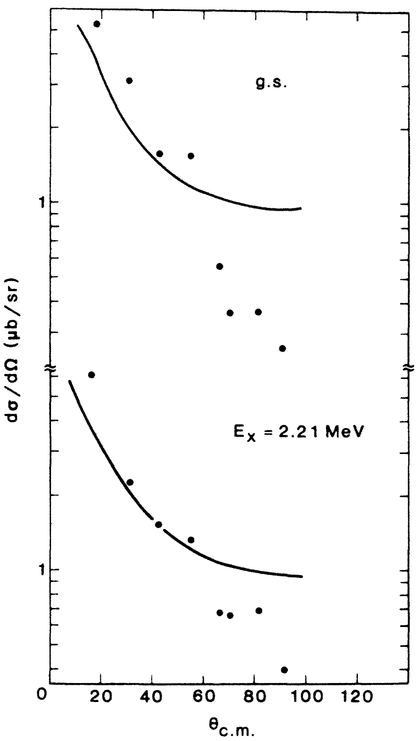

FIG. 7. Angular distributions for the ground state and $E_x = 2.21$ MeV state in ^{27}Al from the ^{12}C(^{19}F,α)^{27}Al reaction, averaged over $\Delta E_{c.m.} = 6$ MeV. The solid curve is the cross section predicted from Hauser-Feshbach calculations over the same average energy interval.

TABLE III. Level density parameters used in the Hauser-Feshbach calculation. a denotes the level density parameter, Δ denotes the pairing correction, and E_c denotes the cutoff energy below which discrete states were used.

Residual nucleus	a (MeV^{-1})	Δ (MeV)	E_c (MeV)	No. of discrete levels
^{12}C	1.59	5.0	10.9	6
^{19}F	3.2	2.5	4.1	10
^{30}P	3.78	0.0	3.4	11
^{30}Si	3.81	2.5	6.0	13
^{27}Al	4.2	2.5	5.42	17
^{25}Mg	3.68	2.5	3.43	10
^{24}Mg	3.36	5.0	7.9	7
^{23}Na	3.73	2.5	5.6	14
^{15}N	1.24	2.5	8.6	9

V. CONCLUSIONS

Statistical analysis of the data obtained in the ^{12}C(^{19}F,α)^{27}Al experiment indicates that intermediate width structures observed in the excitation functions are not strongly correlated. Although anomalies in the correlation function are observed outside accepted statistical limits, they do not correlate with the elastic scattering data. Angular distributions of resolved or unresolved residual states have the same slope but not discernible features. Their slope is much steeper than compound nucleus calculations predict. We therefore conclude that within the present study it has not been possible to identify unequivocally any resonances in the ^{12}C+^{19}F system.

[1]C. F. Maguire, G. L. Bomar, L. Cleeman, J. H. Hamilton, R. B. Piercey, J. C. Peng, N. Stein, and P. D. Bond, Phys. Rev. Lett. **53**, 548 (1984).

[2]P. Braun-Munzinger, in *Proceedings of the International Conference of Heavy-Ion Physics and Nuclear Physics, Catania, Italy, 1983* (North-Holland, Amsterdam, 1983).

[3]S. Kahana, J. Barrette, E. Berthier, E. Chavez, A. Greiner, and M. C. Mermaz, Phys. Rev. C **28**, 1393 (1983).

[4]D. Shapira, R. Novotny, Y. D. Chan, K. A. Erb, J. L. C. Ford, J. C. Peng, and J. D. Moses, Phys. Lett. **114B**, 111 (1982).

[5]D. Pocanic, R. Caplar, G. Vourvopoulos, and X. Aslanoglou, Nucl. Phys. **A444**, 303 (1985).

[6]K. Penney, private communication; L. C. Dennis, A. Roy, A. D. Frawley, and K. W. Kemper, Nucl. Phys. **A359**, 455 (1981).

[7]T. Tachikawa *et al.*, Phys. Lett. **139B**, 267 (1984).

[8]J. Sromicki *et al.*, Nucl. Phys. **A406**, 390 (1983).

[9]C. M. Perey and F. G. Perey, At. Nucl. Data Tables **17**, 1 (1976).

[10]J. Lega and P. C. Macq, Nucl. Phys. **A218**, 429 (1974).

[11]R. Balzer *et al.*, Nucl. Phys. **A293**, 518 (1977).

[12]R. A. Broglia and A. Winther, in *Heavy Ion Reactions* (Benjamin/Cummings, Reading, Mass., 1981), Vol. 1.

[13]C. L. Woods, B. A. Brown, and N. A. Jelley, J. Phys. G **8**, 1699 (1982).

[14]G. E. Moore, K. W. Kemper, and L. A. Charlton, Phys. Rev. C **11**, 1099 (1975).

[15]D. G. Kovar *et al.*, Phys. Rev. **20**, 1305 (1979).

[16]A. Gilbert and A. G. W. Cameron, Can. J. Phys. **43**, 1446 (1965).

[17]U. Facchini and E. Saetta-Menichella, Energ. Nucl. (Madrid) **15**, 154 (1968).

[18]A. G. W. Cameron and R. M. Elkin, Can. J. Phys. **43**, 1288 (1965).